PERGAMON

Journal of Atmospheric and Solar-Terrestrial Physics 64 (2002) 617–624

Journal of
ATMOSPHERIC AND
SOLAR-TERRESTRIAL
PHYSICS

www.elsevier.com/locate/jastp

Variations in planetary radiation belt fluxes and their radiative observations

I. Roth *, R. Millan, R.P. Lin

Space Sciences Laboratory, University of California, Berkeley, CA 94720, USA

Abstract

The variations in the fluxes of the relativistic electrons in the planetary radiation belts are due to a set of different physical processes which violate one or more of the adiabatic invariants. We survey the mechanisms which break down these invariants and investigate the time scales for the processes and the resulting effects on the observed fluxes. The mechanisms include (a) sudden deformation of the magnetic field configuration, (b) radial diffusion due to low-frequency electromagnetic oscillations, (c) transit-time damping due to fast waves and (d) diffusion due to electromagnetic ion-cyclotron (emic) or whistler waves. It is indicated how the waves which interact resonantly with the relativistic electrons are responsible for enhancement in the radiative spectra of the gyrosynchrotron emissions in the GHz frequency range and the X-ray bremsstrahlung emissions at the MeV energy range. © 2002 Published by Elsevier Science Ltd.

Keywords: Radiation belts; Relativistic electrons; Particle acceleration; X-ray observations

1. Introduction

The electromagnetic response of a planetary magnetosphere is controlled by a core magnetic field which is described by a distorted, shifted and tilted dipole. In this planetary environment, ionized particles participate in several quasi-periodic motions. These motions of charged particles (gyration, bounce and drift), which are determined by the structure of the external magnetic field, generally have very disparate frequencies. Although most of the measurements were done at Earth, all the magnetized planets host radiation belts, as observed by the Voyager satellites; the decay of albedo neutrons ejected from the upper atmosphere by cosmic rays (CRAND), global radial diffusion and local acceleration processes are sources of trapped energetic electrons (and ions). Additionally, in the presence of a strong magnetic field and a large planetary magnetosphere (which allows to accelerate the electrons to very high energies) one expects to observe radiation due to gyrosynchrotron emissions from several planets (Jupiter, Saturn, Neptune, and possibly others). The enhancement of the relativistic electron fluxes in the outer radiation belt poses a serious risk to spacecraft and possibly to future human activity in space; these enhancements depend on the timescale of electromagnetic perturbations, on the characteristic eigen-frequencies of electron dynamics and on the losses due to interaction with the atmosphere, with macroscopic bodies or due to other radiative processes. If the perturbation time scale is much longer than that of the quasiperiodic motion of a particle in planetary field, the corresponding adiabatic invariant is conserved; the respective actions (adiabatic invariants) may be violated by perturbations on different time scales. Such processes may violate one or more invariants while preserving the other(s). We survey the possible candidates which violate the adiabatic invariants, the effects on particle fluxes, and present examples of the ring current losses through detectable radiative processes.

2. Energization mechanisms

An enhancement in the fluxes of magnetically trapped relativistic electrons occurs generally as a result of processes which are initiated by: (i) an external impulse,

* Corresponding author. Tel.: +1-510-643-1837; fax: +1-510-643-8302.

E-mail address: ilan@sunspot.ssl.berkeley.edu (I. Roth).

1364-6826/02/$ - see front matter © 2002 Published by Elsevier Science Ltd.
PII: S1364-6826(02)00020-2

(ii) external catalyst, or (iii) internal source. Mechanism (i) consists of a direct, strong electromagnetic impulse which abruptly deforms the magnetic configuration and energizes the electrons (and protons) by breaking their third invariant when a subset of particles is in phase with a single "coherent" wave (Li et al., 1993) or when they are subjected to a large-amplitude ULF waves (Hudson et al., 1997, 2000). It occurs infrequently and requires a Storm Sudden Commencement (SSC) pulse excited by a fast interplanetary shock wave or intense ULF waves excited by a strong Coronal Mass Ejection (CME) perturbation. Mechanism (ii) applies external perturbations which enhance the radial diffusion of a distribution function with a positive radial gradient, violating the flux (third) invariant by a random walk due to broad-band, small-amplitude, low-frequency electromagnetic perturbations (Schulz and Lanzerotti, 1974; Selesnick and Blake, 1997a). It tends to flatten the distribution $f(L)$, where L denotes the equatorial distance in units of planetary radius, but cannot describe separately the increase at lower L shells which is observed during geomagnetically active periods. Mechanism (iii) applies resonant interaction with higher frequency waves on the order of gyration or bounce timescales which violate one or both of the first two invariants (Summers et al., 1998; Roth et al., 1999). It requires recurrent increase in the power of waves which interact with a seed population of electrons (Smith et al., 1996) and diffuse them in energy and pitch-angle. Additionally, intense, fast Alfven waves may be able to enhance the flux of relativistic electrons by perturbing their parallel motion due to the wave mirror force, thus violating the second invariant (Summers and Ma, 2000).

The loss of the relativistic electrons in the radiation belts is important in the evaluation of the steady state conditions (when the average losses are balanced by the steady radial diffusion); it also forms an important diagnostic method based on observations of electromagnetic emission processes in which the electrons participate. The main loss mechanisms include: (a) precipitation into the loss cone due to pitch-angle scattering by waves when the equatorial pitch-angle is such that the mirror force does not prevent the particle from reaching low altitudes, (b) Coulomb collisions when an electron in a presence of a dense plasma loses a small fraction of its energy to the ambient plasma, (c) X-ray bremsstrahlung when small amount of the electron energy is emitted as a radiation; although actual losses are small, this is an important diagnostic of losses since this radiation is observed by instruments flown on balloons and satellites, (d) Synchrotron radiation when an energetic electron in the presence of a strong magnetic field losses a small fraction of its energy due to gyrosynchrotron radio emissions; this process is observed by radio astronomy antennas. In the solar system the main location of this process occurs at the Jovian magnetosphere, (e) absorption by macroscopic bodies. This loss applies mainly to the outer planets which are surrounded by numerous moons.

The main scientific questions regarding the enhancements in the fluxes of these relativistic electrons are: (1) what are the triggers for the acceleration mechanisms? (2) what are the time scales involved? and (3) what are the detectable loss processes? The analysis of the physical mechanisms must include boundary conditions and may be helped by comparative magnetospheres, since different magnetospheres, due to their structure and size, may render a variety of physical observations.

3. Phase space

Usually there exists a large disparity in the values of the eigenfrequencies which are related to the three adiabatic invariants. The gyration Ω, bounce ω_b and drift ω_d frequencies satisfy $\omega_d \ll \omega_b \ll \Omega$, and the motion of a magnetically trapped particle can be described with the help of the action-angle variables: $\mu, \theta_g; J, \phi_b; \alpha, \beta$, where $\mu = p_\perp^2/2m_o B$ denotes the first adiabatic invariant and θ_g the gyrophase, J is the $\oint p_\parallel \, ds$ action (proportional to the second adiabatic invariant) and ϕ_b the bounce phase related to the bounce frequency; α, β are the Euler potentials, defining the magnetic field line on which the guiding center of the particle is instantaneously located. For a dipole configuration, in spherical coordinates (r, θ, ϕ), $r = LR\sin^2\theta$ and $\alpha = -M_o/L \sim \Phi$ is the "flux" or third adiabatic invariant where M_o is the strength of the planetary dipole and $\beta = \phi$ is the azimuth.

Electric field oscillations are effective in μ, J or α diffusion when they occur on time scales of the gyrofrequency, bounce frequency or corotational and gradient-curvature drifts, respectively. Effectively, due to the different time scales of the eigenfrequencies, perturbations over the longer time scales (lower frequencies) generally will not affect the adiabatic invariant conjugate to the higher eigenfrequency. However, those particles which undergo diffusion due to low-frequency modes can simultaneously interact with the magnetized plasma and undergo additional processes which can affect the higher-frequency adiabatic invariant. Without these additional processes, the modifications in the distribution function due to the violation of any one of the adiabatic invariants J_i is given approximately by

$$\frac{\partial F}{\partial t} = \sum_j \sum_i \frac{\partial}{\partial J_i} \left[D_{ij} \frac{\partial F}{\partial J_j} \right], \tag{1}$$

where J_i denote the three adiabatic invariants and D_{ij} are the components of the diffusion tensor. This Fokker Planck equation determines the diffusion time for the invariant J_i

$$\tau_i \sim J_i^2 / D_{ii}. \tag{2}$$

The violation of an adiabatic invariant occurs when the particle and the wave interact strongly by satisfying a particular resonance condition. For a gyrating particle, the local resonance condition equates the Doppler-shifted frequency with the harmonics of the relativistic gyrofrequency,

$$\omega - k_{\parallel} V_{\parallel} = n\Omega/\gamma. \tag{3}$$

Applying this to the bounce-drift motion, we replace the gyration Ω/γ with the bounce frequency ω_{b}, the parallel wavenumber with the wavenumber for a drift at radius r, l/r, and the parallel velocity with the drifting velocity $\omega_{\mathrm{d}} r$, hence Eq. (3) becomes

$$\omega - l\omega_{\mathrm{d}} = n\omega_{\mathrm{b}}. \tag{4}$$

Eq. (4) describes the resonance condition with either both drift and bounce motion, or with each one separately.

4. Radial diffusion

Radial diffusion is a dominant factor in transferring the electrons across the dipolar field lines. The physical mechanism is based on breaking the flux adiabatic invariant. Since the distribution function generally has a positive gradient in L, the diffusion tends to bring the electrons towards lower L-shells; preservation of the first two invariants increases the energy of the electrons. Due to the different time scales of the three eigenfrequencies, this physical process is almost time independent over the gyro/bounce time scales and the gyro/bounce phases are ignorable coordinates. Therefore the remaining phase space variables include μ, J, α, β and the modifications in the distribution function are given by (Birmingham et al., 1974),

$$\frac{\partial F}{\partial t} + \frac{\partial}{\partial \alpha}(\dot{\alpha} F) + \frac{\partial}{\partial \beta}(\dot{\beta} F) + \frac{\partial}{\partial \mu}(\dot{\mu} F) + \frac{\partial}{\partial J}(\dot{J} F) = S(\alpha, \beta, \mu, J, t),$$

where S denotes the source term, which is also related to the boundary conditions. The last two terms on the left-hand side denote the degradation due to radiation processes. Performing an ensemble average over time scales longer than azimuthal drift motion results in

$$\frac{\partial \langle F\rangle}{\partial t} + \frac{\partial \langle F\rangle}{\partial \alpha}\langle\dot{\alpha}\rangle + \frac{\partial \langle F\rangle}{\partial \beta}\langle\dot{\beta}\rangle + \frac{\partial}{\partial \mu}(\dot{\mu}\langle F\rangle) + \frac{\partial}{\partial J}(\dot{J}\langle F\rangle)$$
$$= \frac{\partial}{\partial \alpha}\left[D_{\alpha\alpha}\frac{\partial \langle F\rangle}{\partial \alpha}\right] + \frac{\partial}{\partial \alpha}\left[D_{\alpha\beta}\frac{\partial \langle F\rangle}{\partial \beta}\right] + \frac{\partial}{\partial \beta}\left[D_{\beta\alpha}\frac{\partial \langle F\rangle}{\partial \alpha}\right] + \frac{\partial}{\partial \beta}\left[D_{\beta\beta}\frac{\partial \langle F\rangle}{\partial \beta}\right] + \langle S\rangle.$$

We neglect the azimuthal variations $\partial_\beta = 0$, any average cross-shell drift $\langle\dot{\alpha}\rangle = 0$, and the small effect of the radiation on J (i.e. parallel momentum), $\dot{J}F = 0$, and obtain (dropping the averaged notation)

$$\frac{\partial F}{\partial t} + \frac{\partial}{\partial \mu}(\dot{\mu} F) = \frac{\partial}{\partial \alpha}\left[D_{\alpha\alpha}\frac{\partial F}{\partial \alpha}\right] + S.$$

Changing the variables from α to L and lumping the collision term into an effective time scale τ_{coll} results in

$$\frac{\partial F}{\partial t} + \frac{\partial}{\partial \mu}(\dot{\mu} F)_{\mathrm{rad}} = L^2 \frac{\partial}{\partial L}\left[\frac{D_{LL}}{L^2}\frac{\partial F}{\partial L}\right] - \frac{F}{\tau_{\mathrm{coll}}}. \tag{5}$$

Eq. (5) describes the most commonly used equation for radial diffusion. Without collisions and radiation processes it is equivalent to a one-dimensional Eq. (1). The crucial step for solving it requires the parametrization of the diffusion operator D with respect to L and the geomagnetic activity. A direct approach to calculate the changes in the distribution function propagates a large number of electrons in prescribed magnetic fields which are taken either from analytical models or from global MHD simulations (Elkington, 2000). Generally, in the parametrization of Eq. (5) one assumes $D_{LL} = D_{\mathrm{o}} L^m$. For a dipolar background magnetic field the electrostatic and electromagnetic contributions to D_{LL} give $m = 6$, 10, respectively (Falthammar, 1965), while later corrections due to the magnetic activity index Kp were included for electrostatic (Cornwall, 1968) and electromagnetic (Lanzerotti et al., 1978) perturbations. A numerical fit of Eq. (5) to Polar data gave $m = 11.7$ (Selesnick et al., 1997b), while particle simulations with the inclusion of the correction due to a realistic magnetic field were shown to fit $m = 11$ (Elkington, 2000). The large values of m signify that the diffusion slows down significantly at low L values. On the other hand, fit of the Jovian synchrotron radiation at $L = 1.5$ using Eq. (5) points out that at low L-values $m = 1.8$–3.0 (Birmingham et al., 1974; de Pater and Goertz, 1990, 1994) indicating a different coupling with the upper atmospheric turbulence. A terrestrial study with a time-dependent D_{LL} due to the changing outer boundary conditions (Brautigam and Albert, 2000) gave a good fit to the observed electron fluxes at low first adiabatic invariant ($\mu = 100 - 300$ MeV/G), but a significant discrepancy at higher μ values, indicating that an additional process which may violate the first or second adiabatic invariant operates for higher energy electrons.

5. Transit time damping due to fast waves

The L-diffusion may explain the slow increase in the energetic electron distributions (mainly in the equatorial plane) via violating the third adiabatic invariant through a global magnetospheric interaction (e.g. Liu et al., 1999). The time scales involved depend on the amplitudes of the ULF waves: in most cases it stretches from few days (at Earth) to many months (at Jupiter). Only on rare occasions, like in the case of the 10–11 January 1997 CME magnetic cloud event, was enhanced ULF activity with the drift-resonant acceleration shown as a viable mechanism for the relativistic flux enhancement over shorter time scales (Hudson et al., 2000; Elkington et al., 1999). Since often the time scales related to the enhancements in the fluxes of relativistic electrons are significantly shorter, one may invoke a local interaction (on a given L-shell) between electrons and waves which are excited at a narrow range of the L-shells. One possible wave mode which was used in solar (Miller, 1997) and magnetospheric application (Summers and Ma, 2000) is the low-frequency, compressional, fast magnetosonic, oblique MHD mode with a parallel magnetic component. This interaction between the electron magnetic moment and the parallel gradient of the magnetic field $-\mu\nabla_{\|}B$ may be described as a magnetic analogue of the Landau damping, when the roles of the charge and the electric potential are replaced by μ (first adiabatic invariant) and the absolute value of the total (ambient plus wave-parallel) magnetic field, respectively. The interaction applies mainly to electrons and is strongest when the period of the compression of the parallel magnetic component is equal to the transit time of the electron. In the frame of the wave the particles are reflected by the compression; in the plasma frame it is equivalent to head-on or trailing collisions, similarly to Fermi acceleration.

This interaction violates the second adiabatic invariant. For oblique waves the $n = 0$ resonance condition (Eq. (3)) can be easily satisfied for the tail of the electron distribution and together with the fast-mode dispersion relation $\omega = kV_A$ results in a validity condition for the threshold energy E_{th},

$$E > E_{th} \sim \beta_A^2/2.$$

where β_A is the Alfven speed in units of c. The calculated time scale $\tau \sim p^2/D(p)$ (Eq. (2)) results in an energization of substorm-related injected electrons at 100–200 keV (Smith et al., 1996) to the observed MeV fluxes in several hours (Summers and Ma, 2000).

6. Diffusion due to whistler waves

Another natural candidate for acceleration of the energetic electrons which bounce along magnetic field lines is oblique whistler waves. These magnetospheric whistler waves acquire significant oblique wavenumbers along their paths due to the changing magnetic field and density profile (Thorne and Horne, 1994) and therefore are able to interact resonantly at several regular and anomalous gyroharmonic resonances. The interaction at higher and anomalous gyroharmonics is particularly efficient for relativistic particles with gyroradii of the order of the whistler wavelengths. This interaction violates the first and the second adiabatic invariants, and the resulting diffusion in pitch-angle and in energy results in a hardening of the spectrum of the relativistic electrons over time-scales much shorter than those related to the L-diffusion.

The mechanism involves resonant interaction with electrons bouncing and gyrating along the inhomogeneous dipole magnetic field, $\omega - k_{\|}v_{\|} - n\Omega/\gamma \sim 0$, where the wave is characterized by its frequency ω and parallel wavenumber $k_{\|}$ and the resonating electron by its parallel velocity $v_{\|}$, local gyrofrequency Ω and the relativistic factor γ, while the integer n denotes the harmonic of the cyclotron interaction. For the high harmonic interaction the wave frequency is much smaller than the harmonics of the gyrofrequency and the resonance involves effectively the gyrofrequency, parallel wavenumber and parallel velocity. Therefore, electromagnetic ion-cyclotron waves (emic) are also able to resonate with the relativistic electrons (Horne and Thorne, 1998).

Fig. 1 describes (a) the temporal evolution of the kinetic energy $W = mc^2(\gamma - 1)$, (b) the first adiabatic invariant μ, (c) the equatorial pitch-angle α' (related to the second adiabatic invariant), over a few bounce periods (6.0 s) and the first few electron resonance crossings. μ is calculated by its lowest order approximation at the electron position: $p_\perp^2/2m_oB(x)$, while α' is calculated by adiabatically projecting the instantaneous pitch-angle to the equator ($z = 0$) with the help of the momenta $(p_z, p_\perp)$: $\alpha' = tg^{-1}\{p_\perp/[p_\perp^2(z/D)^2 + p_z^2(1+(z/D)^2)]^{1/2}\}$. Fig. 1(d) shows the calculated normalized resonance criterion $v(t) = [\gamma(t)\omega - k_{\|}(z)p_{\|}(t)]/\Omega(x(t))$. When $v(t)$ approaches an integer, strong interaction may be expected. The equatorial magnetic field is 0.01 gauss, $E_o = 1$ mV/m and $k_\perp = 10$ km^{-1} and the propagating wave satisfies the local dispersion relation. Between resonances ($v(t)$ not too close to an integer n) the electron moves adiabatically, i.e. both adiabatic invariants are constant as seen in segments of Fig. 1, but when it crosses a resonant region (v approaches an integer n), an irreversible change in energy, in first adiabatic invariant and in equatorial pitch-angle may occur. One observes that the electron performs a random walk in all quantities. Because the resonant interactions include a variety of positive and negative values of n, changes in energy and in pitch-angle are not correlated. Additionally, in contrast to the energy and the equatorial pitch-angle (second adiabatic invariant), the first adiabatic invariant, which depends only on the perpendicular momentum, is not affected by the $n = 0$ resonance. The time scale for modifications in the distribution function may be as low as tens of minutes (Roth et al., 1999).

7. Radiative loss mechanisms

Generally, the life time of relativistic electrons is quite long. For instance, the low-orbiting MIR station with its large geometrical factor, was still able to detect the MeV electrons which were injected in the strong March 1991 event as a result of SSC, almost a decade later. Some of the loss mechanisms for the radiation-belt electrons can be used for diagnostic purposes. Here we discuss two diagnostic methods for the interacting electrons which can be observed remotely via incoherent electromagnetic radiation.

7.1. Gyrosynchrotron emissions of relativistic electrons

Since the discovery of radio emission from Jupiter (Burke and Franklin, 1955) it is widely accepted that the Jovian radio waves can be classified according to their frequency

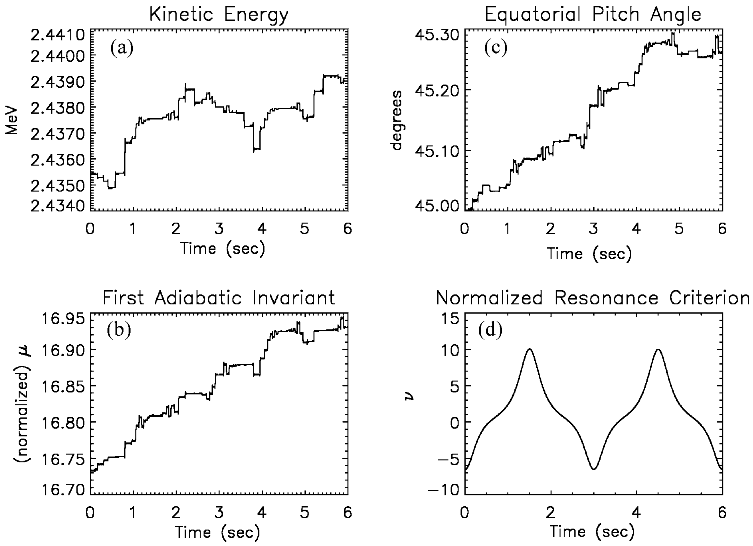

Fig. 1. Temporal evolution of (a) relativistic kinetic energy W, (b) first adiabatic invariant μ, (c) equatorial pitch-angle α' and (d) resonance criterion v. $B_{eq} = 0.01$, $D = 100\,000$ km, $E_o = 1$ mV m^{-1}, $k_\perp = 10$ km^{-1}, density $= 10$ cm^{-3}. Initial pitch-angle $\alpha'_o = 45^\circ$, initial gyrophase $\delta_o = 45^\circ$.

as decametric ($<$ 40 MHz) due to cyclotron emissions and decimetric (0.1–15 GHz) due to synchrotron radiation, with a thermal component at its higher end. The Jovian synchrotron radiation is seen at Earth above the galactic noise level due to its strong magnetic field (4.28 G at the equator) and a sufficiently intense flux of energetic electrons (greater than few MeV). This radiation, known for a long time (e.g. Radhakrishnan and Roberts, 1960; Morris and Berge, 1962) was used in determining the inclination of the magnetic dipole field with respect to the rotational axis, as well as the magnitude of the multipole correction to the field (Warwick, 1963). The theory of radio emission by relativistic electrons is believed to account for many observed emissions from a variety of cosmic sources (e.g. Ginzburg and Syrovatskii, 1964). The full description of the synchrotron emission in the presence of strong magnetic field includes the effects of ambient medium and reabsorption by the radiating electrons themselves (e.g. Ramaty, 1969; Ramaty et al., 1994). In the presence of magnetized plasma the radiation may propagate at different modes (ordinary O and extraordinary X) and for a Lorentz factor γ below the plasma-to-gyro frequency ratio, the emissions at low frequencies are substantially suppressed (Razin effect). The reabsorption affects the wave power spectrum and modifies the polarization of the resultant radiation.

The increase in the intensity of the radio emissions is related to the enhancement in the fluxes of relativistic electrons, i.e. to the violation of adiabatic invariants. The changes in the adiabatic invariants due to the interaction with the waves depend on the (random) phases at the entry into the resonant region; successive resonant interactions form a stochastic process. The distribution function of the seed electrons generally decreases with energy and increases with L and the main manifestation of the diffusion process, which involves expansion into the lower-density region of the phase space, may be seen as an increased flux at higher energies and lower L values. An analysis of resonant dispersion curves for parallel propagating whistler waves showed that the diffusion results in a κ distribution with a significant tail (Ma and Summers, 1998). For general oblique propagation the different resonances between electrons and whistler waves are not correlated, hence their stochastic interaction will also result in tail enhancement. Therefore, an enhancement in radio emissions may be related to a flattening of electron distribution function, i.e. lowering of the power-law index. The calculated emissions can be compared to observations.

Figs. 2(a)–(b) and (c)–(d) show the gyrosynchrotron emissivity of the radio emission and the absorption coefficients, respectively, as a function of frequency (in units of the gyrofrequency). The distribution of electrons was taken as a power-law in energy $g(E) = N_o E^{-\psi}$ with an index $\psi = 2.5$, while the angle between the magnetic field and the line of sight Θ was taken arbitrarily as 45°. The magnetic field is assumed constant at $B = 1$ gauss, i.e. the calculations describe, for example, emission from a high-latitude, low-L region. The source size was taken as a small fraction of the flux tube. The calculations perform a summation of many terms with Bessel functions over both modes of propagation, resulting in oscillatory behaviour at the lower part of the spectrum. Above the transition energy of 10 MeV (which satisfies the electron energy to be much higher than

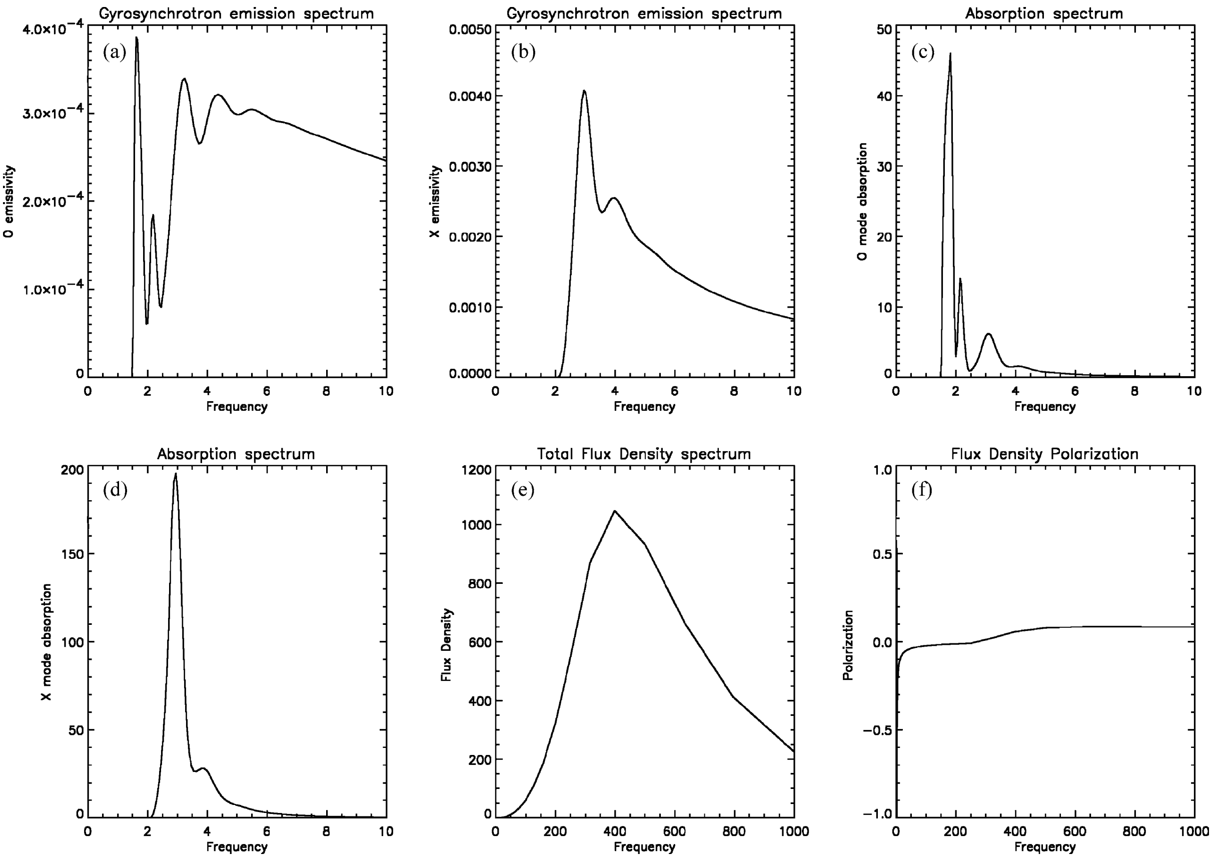

Fig. 2. Radio spectral emission for electron distribution with a power-law $\psi = 2.5$ and magnetic field $B = 1$ G. (a), (b) O/X emissivities; (c), (d) O/X absorption coefficients; (e) total flux density; (f) polarization. The frequency is given in units of the gyrofrequency. Note the varying spectral range.

its rest energy) the calculations use the ultrarelativistic approximation (Ginzburg and Syrovatskii, 1965). Since the radiation can be reabsorbed by the plasma the radio emission spectrum is significantly different from the spectrum of emissivity. Fig. 2(e) presents the total flux density spectrum observed at Earth (first Stokes parameter), normalized to the total electron number $g(E)$. One observes that the peak occurs at high harmonic and the spectrum extends to very high harmonics of the gyrofrequency (for $B = 1$ G the value of the highest plotted frequency is 2.8 GHz). Enhancement of this radiation is a direct result of the resonant interaction with either ULF or whistler waves.

7.2. Hard X-ray bursts

Energetic electrons which are pitch-angle diffused into the loss cone and are able to reach low altitudes and interact with the dense atmosphere are observed through the X-ray emissions at balloon altitudes of 40 km. While the electrons lose most of their energy via Coulomb collisions, the Bremsstrahlung is the most important observational method for their detection. Balloons form a stationary platform for observations of a particular field line (in contrast to the satellites which cross the field lines with a velocity of $\sim$ 10 km s^{-1}); they were the first to observe X-ray emissions due to precipitating electrons into the atmosphere (Winckler et al., 1958). Only recently the first measured MeV X-ray spectra from a terrestrial source were obtained with balloon-borne instruments (August 1996, near Kiruna, Sweden) (Foat et al., 1998). In an 18 day balloon flight around Antarctica the same instruments detected 7 MeV X-ray bursts demonstrating that they are not uncommon.

The analysis of the event amounts to a deconvolution of the electron energy spectrum and flux from the observed X-ray spectra. The bremsstrahlung cross-section is well known and one can simulate the electron Coulomb as well as photon Compton scattering for a given source of electron distribution all the way to the balloon instrument. The measured spectra with and without instrument and atmospheric response corrections are shown in Fig. 3, together with a fit assuming a δ function at 1.7 MeV for the electron source. A power-law electron distribution does not fit the

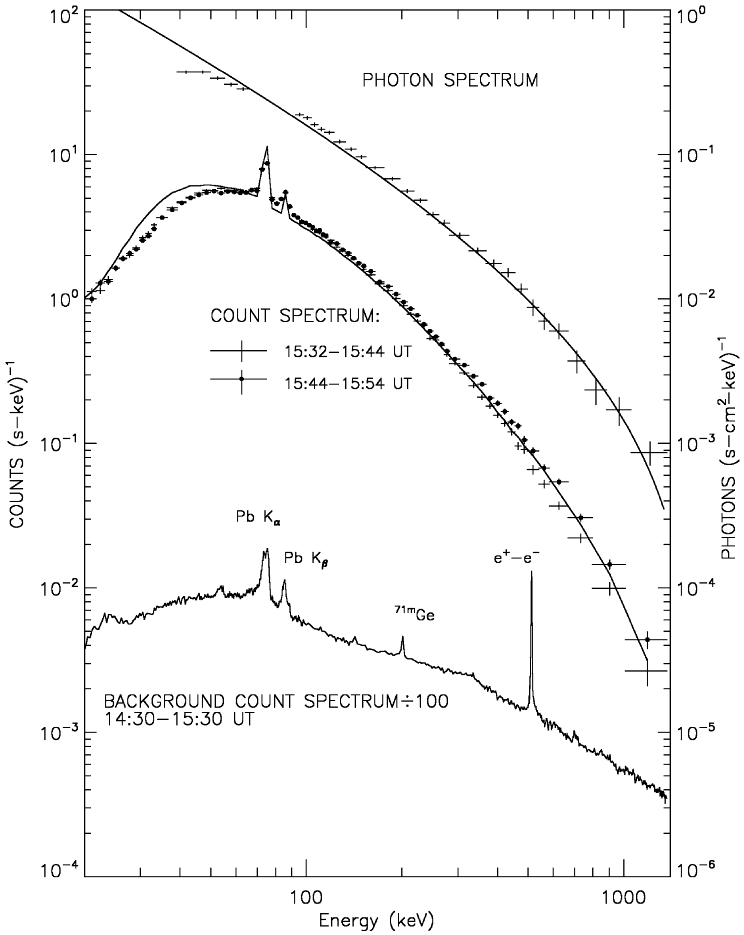

Fig. 3. Background count spectrum (bottom), the measured count spectrum, and deconvolved photon spectrum (crosses) and the model spectrum (solid lines) assuming an electron δ function at 1.7 MeV.

data, indicating that the radiation-belt electrons are selectively diffused by a particular set of waves. Recent analysis (Lorentzen et al., 2000) showed that parallel whistler waves cannot satisfy the required condition for resonance with the energetic electrons, while emic waves can satisfy it, provided the plasma density is above 10 cm^{-3}.

8. Summary

The changes in the fluxes of relativistic electrons, trapped in a planetary magnetic field, require violation of one or more of the adiabatic invariants. These invariants describe the quantities which are approximately conserved while the charged particle performs one of the quasi-harmonic motions. The violation of an invariant occurs when it encounters waves such that the (Doppler shifted) frequency of the wave is close to the eigenfrequency of the wave mode. Two examples of a resonant interaction between coherent electromagnetic waves and observation of incoherent radiation due to the modified electron distribution function show that the resonant processes affecting the radiation-belt electrons can be monitored remotely. Understanding of the processes which determine the behaviour and evolution of the radiation belts is crucial for future space investigation.

Acknowledgements

The authors acknowledge the support by NASA grants NAG5-9626, NAG5-8078, NGT5-30110, NAG5-6928, NAG5-9975 and NAG5-3596.

References

Birmingham, T., Hess, W., Northrop, T., Baxter, R., Lojko, M., 1974. The electron diffusion coefficient in Jupiter's magnetosphere. Journal of Geophysical Research 79, 87.

Brautigam, D.H., Albert, J.M., 2000. Radial diffusion analysis of outer radiation belt electrons during the October 9, 1990, magnetic storm. Journal of Geophysical Research 105, 291.

Burke, B.F., Franklin, K.L., 1955. Observations of a variable radio source associated with the planet Jupiter. Journal of Geophysical Research 60, 213.

Cornwall, J.M., 1968. Diffusion processes influenced by conjugate-point wave phenomena. Radio Science 3, 740.

de Pater, I., Goertz, C.K., 1990. Radial diffusion models of energetic electrons and Jupiter's synchrotron radiation: Steady state solution. Journal of Geophysical Research 95, 39.

de Pater, I., Goertz, C.K., 1994. Radial diffusion models of energetic electrons and Jupiter's synchrotron radiation: Time variability. Journal of Geophysical Research 99, 2271.

Elkington, S.R., Hudson, M.K., Chan, A.A., 1999. Acceleration of relativistic electrons via drift-resonance interaction. Geophysical Research Letters 26, 3273.

Elkington, S.R., 2000. Ph.D. Thesis, Dartmouth College.

Falthammar, C.-G., 1965. Effects of time-dependent electric fields on geomagnetically trapped radiation. Journal of Geophysical Research 70, 2503.

Foat, J.E., et al., 1998. First detection of a terrestrial MeV X-ray burst. Geophysical Research Letters 25, 4109.

Ginzburg, V.L., Syrovatskii, S.I., 1965. Annual Review of Astronomy and Astrophysics 3, 297.

Ginzburg, V.L., Syrovatskii, S.I., 1964. The origin of Cosmic Rays. Macmillan Co., New York.

Horne, R.B., Thorne, R.B., 1998. Potential waves for relativistic electron scattering and stochastic acceleration during magnetic storms. Geophysical Research Letters 25, 3011.

Hudson, M.K., Elkington, S.R., Lyon, J.G., Goodrich, C.C., Rosenberg, T.J., 1997. Simulation of radiation belt formation during storm sudden commencement. Journal of Geophysical Research 102, 14 087.

Hudson, M.K., Elkington, S.R., Lyon, J.G., Goodrich, C.C., 2000. Increase in relativistic electron fluxes in the inner magnetosphere. Advances in Space Research 25, 2327.

Lanzerotti, L.J., Webb, D.C., Arthur, C.W., 1978. Geomagnetic field fluctuations at synchronous orbit: radial diffusion. Journal of Geophysical Research 83, 3866.

Li, X., Roth, I., Temerin, M., Wygant, J.R., Hudson, M.K., Blake, J.B., 1993. Simulation of the prompt energization and transport of radiation belt particles during the March 24, 1991 SSC. Geophysical Research Letters 20, 2423.

Liu, W.W., Rostoker, G., Baker, D.N., 1999. Internal acceleration of relativistic electrons by large-amplitude ULF pulsations. Journal of Geophysical Research 104, 17 391.

Lorentzen, K.R., et al., 2000. Precipitation of relativistic electrons by interaction with emic. Journal of Geophysical Research 105, 5381.

Ma, C., Summers, D., 1998. Formation of Power-law Energy Spectra in Space Plasmas by Stochastic Acceleration due to Whistler-Mode Waves. Geophysical Research Letters 25, 4099.

Miller, J.A., 1997. Electron acceleration in solar flares by fast mode waves. Astrophysics Journal 491, 939.

Morris, D., Berge, G.L., 1962. Measurements of the polarization and angular extent of the decimetric radiation of Jupiter. Astrophysics Journal 136, 276.

Radhakrishnan, V., Roberts, J.A., 1960. Polarization and angular extent of the 960 Mc/sec radiation from Jupiter. Physical Review Letters 4, 493.

Ramaty, R., 1969. Astrophysics Journal 158, 753.

Ramaty, R., Schwartz, R.A., Enome, S., Nakajima, H., 1994. Gamma-ray and millimeter-wave emissions from the 1991 June X-class solar flares. Astrophysics Journal 436(2), 941.

Roth, I., Temerin, M., Hudson, M.K., 1999. Resonant enhancement of relativistic fluxes during geomagnetically active periods. Annals of Geophysics 17, 631.

Schulz, M., Lanzerotti, L.J., 1974. Particle Diffusion in the Radiation Belts. Springer, New York, 215pp.

Selesnick, R.S., Blake, J.B., 1997a. Dynamics of the outer radiation belts. Geophysical Research Letters 24, 1347.

Selesnick, R.S., Blake, J.B., Kolasinski, W.A., 1997b. A quiescent state of 3–8 MeV radiation belt electrons. Geophysical Research Letters 24, 1343.

Smith, A.J., Freeman, M.P., Reeves, G.D., 1996. Postmidnight VLF chorus events, a substorm signature observed at the ground near $L = 4$. Journal of Geophysical Research 101, 24 641.

Summers, D., Thorne, R.M., Xiao, F., 1998. Relativistic theory of wave-particle resonant diffusion with applications to electron acceleration in the magnetosphere. Journal of Geophysical Research 103, 20 487.

Summers, D., Ma, C., 2000. Rapid acceleration of electrons in the magnetosphere by fast-mode MHD waves. Journal of Geophysical Research 105, 15887.

Thorne, R.M., Horne, R.B., 1994. Landau Damping of Magnetospherically Reflected Whistlers. Journal of Geophysical Research 99, 17 249.

Warwick, J.W., 1963. The position and sign of Jupiter magnetic moment. Astrophysics Journal 137, 1317.

Winckler, J.R., Peterson, L., Arnoldy, R., Hoffman, R., 1958. X-rays from visible aurorae. Physica Review 110, 1221.